

## Crystal structure of tilleyite: Refinement and coordination

By S. J. LOUISNATHAN\* and J. V. SMITH

Department of the Geophysical Sciences, University of Chicago  
Chicago, Illinois

(Received June 15, 1970)

### Auszug

Die Atom-Parameter eines natürlichen Tilleyits wurden nach dem dreidimensionalen Ausgleichs-Verfahren verfeinert. Die Verformungen der Kolonnen von Calcium-Sauerstoff-Oktaedern lassen sich meistens durch Verkürzung der gemeinsamen Kanten erklären. In der  $\text{Si}_2\text{O}_7$ -Gruppe sind die Längen der (Si–O)-Brücken-Bindungen 1,656(7) und 1,678(7) Å, die der peripheren Bindungen 1,602(7) und 1,616(7) Å; der Si–O–Si-Brücken-Winkel beträgt 157°. Die inneren (O–O)-Kanten (Mittel: 2,58 Å) sind kürzer als die äußeren Kanten (Mittel: 2,71 Å); dies ist verträglich mit den Coulomb-Kräften in der  $\text{Si}_2\text{O}_7$ -Gruppe und mit einem  $\pi$ -Bindungs-Mechanismus.

### Abstract

The atomic parameters of a natural tilleyite [ $a = 15.108(3)$ ,  $b = 10.241(1)$ ,  $c = 7.579(1)$  Å,  $\beta = 105.17(1)^\circ$ ] were refined by least squares using three-dimensional data. The distortions of the columns of calcium-oxygen octahedra are mostly explainable by shortening of shared edges. In the  $\text{Si}_2\text{O}_7$  group the Si–O bridge bonds are 1.656(7) and 1.678(7) Å and the peripheral bonds are 1.602(7) and 1.616(7) Å and the bridging Si–O–Si angle is 157°. The inner O–O edges (average 2.58 Å) are shorter than the outer edges (average 2.71 Å), consistent with Coulombic forces in the  $\text{Si}_2\text{O}_7$  group and with a  $\pi$ -bonding mechanism.

### Introduction

The crystal-structure determination by SMITH (1951, 1953) of tilleyite,  $\text{Ca}_5\text{Si}_2\text{O}_7(\text{CO}_3)_2$ , was incomplete because the primitive level of experimental and computational facilities made it necessary to use two-dimensional projections. Since tilleyite has a strong pseudo structure, the two-dimensional refinement resulted in averaging of some atomic coordinates which obscured details of the structure.

\* Present address: Department of Geological Sciences, Virginia Polytechnic Institute and State University, Blacksburg, Virginia 24061.

A new three-dimensional refinement using intensities collected with an automatic diffractometer has now been made. The interatomic distances are discussed using recent ideas on the nature of chemical forces.

The original description of the crystal structure by SMITH was improved by BELOV (1963) who recognized tilleyite as the prototype of a series of structures. Common to these structures is a corrugated wall of linked calcium-oxygen octahedra and  $\text{Si}_2\text{O}_7$  groups (*corrugated wall* is geometrically more accurate than the term *ribbon* used in the English translation of Belov's work).

### Experimental

The cell dimensions and standard errors of tilleyite obtained for three specimens are as follows:

$a$	$b$	$c$	$\beta$	
15.111(5) Å	10.242(2) Å	7.577(2) Å	105.15(2)°	natural specimen from Barnavave, Carlingford, Ire- land.
15.079(10)	10.241(4)	7.573(3)	105.14(3)	synthetic specimen kindly supplied by Dr. R. I. HARKER of Tempres, Inc.
15.108(3)	10.241(1)	7.579(1)	105.17(1)	natural specimen from Crestmore, California, U.S.A.

X-ray powder diffractometer patterns calibrated with pure silicon ( $a = 5.43062$  Å) as internal standard were made of the samples and the above cell dimensions were obtained by least-squares adjustment of  $1/d^2$  values using a program written by C. W. BURNHAM. A completely indexed powder pattern will be published in the Powder Diffraction File.

A single crystal was selected from Crestmore material kindly supplied by Dr. PAUL B. MOORE. A cleavage fragment of  $0.007 \text{ mm}^3$  volume was mounted on the  $b$  axis. Fourteen levels of three-dimensional data up to a limit of  $2\theta = 80^\circ$  were collected with a PAILRED automatic diffractometer using monochromatic  $\text{MoK}\alpha$  radiation. Of the 6067 independent reflections, 1920 had zero intensity, including



Table 1. (Continued)

Table with columns for h k l, F\_o, F\_c, and multiple rows of numerical data representing crystal structure parameters.







Table 1. (Continued)

<i>hkl</i>	$F_o$	$F_c$	<i>hkl</i>	$F_o$	$F_c$	<i>hkl</i>	$F_o$	$F_c$	<i>hkl</i>	$F_o$	$F_c$	<i>hkl</i>	$F_o$	$F_c$	<i>hkl</i>	$F_o$	$F_c$
-8 12 9	12.5	13.0	-9 13 1	8.3	8.6	-12 13 3	5.0	5.8	6 13 6	9.9	8.0	8 14 0	6.5	6.2	10 14 2	6.1	5.2
-14	5.2	6.0	-10	7.9	8.1	-13	8.6	11.0	-7	6.0	4.6	-8	7.2	6.2	-10	12.3	16.5
0 12 10	32.5	31.0	15	5.7	4.7	14	6.3	4.9	-8	18.2	28.0*	9	26.4	25.6	11	10.8	9.7
-2	4.7	5.4	4	4.2	9.7	15	7.4	8.8	-9	14.3	14.7	-9	24.0	25.6	12	8.6	13.6
-3	9.0	7.8	17	5.7	2.0	-17	6.3	8.9	10	13.4	11.3	10	11.7	10.9	13	6.5	5.3
-4	6.6	6.1	-18	5.2	6.0	0 13 4	30.9	30.3	-10	5.7	7.9	-10	11.1	10.9	-13	8.7	12.7
-6	14.7	14.3	0 13 2	21.7	21.1	-1	5.3	4.3	-11	14.2	16.7	12	8.2	6.8	-14	9.3	12.3
-8	5.5	4.8	1	15.5	15.2	1	11.7	10.8	-16	5.7	7.5	-12	7.5	6.8	-15	8.9	8.7
-10	12.1	11.6	-1	13.4	14.2	2	11.4	11.0	-17	11.7	11.8	13	10.7	10.1	-17	6.6	7.2
2 13 0	40.1	40.5	-2	26.1	26.7	-2	4.2	3.4	0 13 7	13.9	13.3	-13	9.2	10.1	0 14 3	5.9	6.0
-2	38.9	40.5	3	16.7	15.0	3	30.5	28.4	-1	6.5	6.3	14	5.1	3.8	1	3.9	4.3
3	14.1	13.4	5	15.8	16.7	-4	36.3	35.0	5	5.6	5.4	15	4.9	4.6	-1	3.5	2.7
-3	13.7	13.4	4	13.4	23.3*	5	14.1	12.1	-5	8.8	8.8	16	15.7	15.2	3	9.6	8.7
4	14.9	14.2	5	10.5	7.8	-5	10.5	11.9	6	5.2	3.0	-16	14.0	15.2	-5	10.7	10.5
-4	15.0	14.2	-5	6.7	6.4	6	4.9	4.3	-7	13.3	15.0	17	5.9	4.5	6	13.8	11.8
-5	36.5	36.1	6	11.0	9.1	-6	14.7	15.1	-9	6.4	5.7	-17	5.7	4.5	-6	8.2	8.8
-5	36.1	36.1	-6	24.2	28.1	7	6.8	4.6	-11	6.8	6.1	1 14 1	14.6	13.0	7	8.5	6.9
6	12.2	11.7	7	31.2	26.0	-7	22.5	25.1	-13	9.5	9.1	-1	2.2	4.9	-7	4.4	3.4
-6	11.7	11.7	-7	18.4	18.2	8	3.7	5.2	-14	5.8	5.9	4	7.8	10.7	-8	3.9	3.1
7	21.8	20.8	-8	9.1	9.7	-9	12.5	13.5	-15	12.9	15.3	-5	8.0	8.3	10	5.1	2.8
-7	21.4	20.8	-9	28.3	31.0	10	20.2	16.2	-16	4.4	0.3	6	5.7	4.1	11	11.9	9.8
-8	3.7	2.3	10	12.5	11.4	11	12.8	12.2	0 13 8	5.7	3.9	-6	4.0	4.2	-11	5.8	7.3
9	13.9	12.2	-10	7.4	8.7	-11	17.4	17.0	1	15.1	13.9	7	4.3	5.3	13	21.3	18.8
-9	14.1	12.2	11	6.6	3.9	12	9.7	10.9	-1	8.3	8.2	-8	7.9	15.2*	-13	4.3	7.4
10	6.2	5.6	12	8.3	9.5	-13	13.7	15.5	-2	15.0	15.0	-9	6.6	7.1	14	12.3	11.1
-10	5.2	5.6	-13	6.3	4.7	14	8.3	7.7	-3	9.2	9.6	10	5.2	6.5	-16	6.9	7.5
11	6.7	7.3	14	26.1	22.6	-15	8.0	9.1	-5	4.0	1.7	-10	4.1	2.8	0 14 4	6.9	9.0
-11	7.1	7.3	-14	5.8	7.2	-1 13 5	10.5	10.4	-6	18.6	19.1	11	14.7	14.9	1	18.3	18.3
12	9.7	10.0	15	11.7	11.8	-2	3.2	2.7	-7	12.5	14.3	14	7.8	6.7	-1	12.5	11.7
-12	10.3	10.0	-15	5.1	3.4	-5	14.0	14.9	-8	10.5	10.2	15	7.5	7.8	-2	30.5	29.7
13	8.7	9.5	16	10.7	7.3	4	14.3	15.2	-9	7.5	9.6	-15	9.9	12.4	3	6.4	6.0
-13	9.4	9.5	-17	6.5	8.4	-5	5.2	5.2	-11	5.2	4.6	-16	2.9	6.4	4	19.2	17.6
14	7.9	8.5	0 13 3	3.6	6.1	7	9.1	7.4	-12	9.3	9.7	-17	5.8	4.6	-6	4.3	3.5
-14	7.8	8.5	1	8.9	7.9	-7	5.6	5.7	-13	10.4	10.1	1 14 2	3.5	1.2	7	22.1	19.3
16	5.4	5.9	-1	5.3	5.2	9	8.8	6.7	-14	5.8	5.5	-1	7.5	6.8	-7	14.9	15.3
18	16.9	16.3	2	17.7	16.1	-9	12.7	13.2	-5 13 9	9.7	10.5	2	34.9	31.3	8	14.1	11.6
-18	15.8	16.3	-2	4.0	2.3	-10	7.4	8.0	-6	9.5	10.7	-2	4.9	5.0	-8	23.1	27.6
0 13 1	3.6	3.3	3	5.7	5.9	11	14.0	11.9	-8	6.7	6.7	3	24.1	19.9	-9	7.1	12.6
1	4.1	4.9	-3	7.1	6.1	-11	11.5	13.4	-9	4.5	6.1	-3	8.0	7.0	11	10.0	9.0
-1	12.7	13.5	4	6.3	6.0	-12	2.5	5.3	2 14 0	8.0	9.7	-4	37.0	36.6	-11	13.0	16.8
-2	7.2	11.3	-5	15.6	16.3	-14	5.1	6.0	-2	8.9	9.7	5	27.8	29.3	12	6.0	5.3
3	9.5	8.5	-6	8.1	9.5	-17	5.7	6.0	3	21.5	20.8	-5	16.1	15.1	13	5.0	8.2
-3	7.7	8.4	-7	9.3	8.6	0 13 6	5.1	1.8	-3	20.9	20.8	6	10.9	8.6	-14	9.7	11.3
4	8.6	4.0	-8	9.3	11.6	1	10.8	10.9	5	7.0	6.1	-6	12.0	13.3	-15	8.4	10.0
5	6.7	5.5	9	8.2	6.7	-1	8.9	9.4	-5	5.7	6.1	7	11.8	9.3			
6	17.3	17.4	-9	3.8	2.0	2	12.5	11.9	6	26.7	26.3	-7	21.2	25.0			
-6	5.0	5.7	-10	3.9	3.4	-2	13.2	13.4	-6	25.4	26.3	8	6.3	11.0			
-7	9.6	9.7	11	6.9	7.1	-3	17.5	17.7	7	11.7	10.2	9	8.6	8.2			
-8	5.6	7.0	-11	6.9	6.8	5	15.7	13.8	-7	11.2	10.2	-9	7.9	9.7			

the space-group extinctions for  $P2_1/a$ . The remaining 4147 data were corrected for Lorentz and polarization effects. An absorption correction for polyhedral transmission was applied using C. W. BURNHAM's subroutines ABSRP1 and ABSRP2.

The structure was refined with  $P2_1/a$ , using the SORFLS program. All  $hkl$  data with  $k = 3$  were omitted from the calculations since an instrumental setting error was detected for this level. This left 3589 non-zero data for the 103 variable parameters comprising individual scale factors for each  $k$  level, 66 atomic positional and 22 isotropic thermal vibrational parameters and an extinction parameter (after ZACHARIASEN, 1963*a*). After six cycles of refinement with a single scale factor and unit weights for all data the agreement factor dropped to 0.18 from a starting value of 0.23. Introducing anomalous correction terms for Ca and Si (values of  $f'$  and  $f''$  from CROMER, 1965) and individual scale factor for each  $k$  layer the agreement factor fell to 0.16 in three further cycles. The residuals correlated with  $F_{\text{obs}}$  and not with  $(\sin \theta)/\lambda$ . Omitting nine very strong and 130 medium to weak reflections that showed very large residuals from the beginning, and introducing

$$w(hkl) = 1.0/[20.0 + F_{\text{obs}}(hkl) + 0.01 F_{\text{obs}}^2(hkl)]$$



Table 2  
*Fractional atomic coordinates and thermal vibrational parameters in tilleyite*

Atom	<i>x</i>	<i>y</i>	<i>z</i>	<i>B</i>
Ca(1)	0.0033(1)	0.9938(2)	0.7501(3)	0.75(2)
Ca(2)	0.1769(1)	0.2135(2)	0.0908(2)	0.69(2)
Ca(3)	0.1813(1)	0.2064(2)	0.6087(2)	0.79(2)
Ca(4)	0.1239(1)	0.5895(2)	0.0449(2)	0.62(2)
Ca(5)	0.1359(1)	0.5787(2)	0.5599(2)	0.72(2)
Si (1)	0.2032(1)	0.9209(2)	0.1381(3)	0.42(3)
Si (2)	0.2023(1)	0.9142(2)	0.5689(3)	0.57(3)
C (1)	0.0301(6)	0.3058(9)	0.3402(11)	1.14(12)
C (2)	0.0248(6)	0.3018(9)	0.8157(11)	0.84(11)
O (1)	0.0752(5)	0.2084(8)	0.2983(10)	1.10(10)
O (2)	0.0713(5)	0.2052(8)	0.7867(10)	1.08(10)
O (3)	0.0705(4)	0.3772(7)	0.4807(9)	1.08(10)
O (4)	0.0547(4)	0.3766(7)	0.9563(9)	1.01(9)
O (5)	0.0519(5)	0.6642(7)	0.7549(10)	1.37(10)
O (6)	0.0584(5)	0.6826(7)	0.2834(10)	1.25(11)
O (7)	0.2253(4)	0.7744(7)	0.0878(8)	0.73(12)
O (8)	0.2272(5)	0.7665(7)	0.6290(8)	0.81(9)
O (9)	0.1008(5)	0.9760(8)	0.0528(9)	0.98(9)
O (10)	0.1018(4)	0.9711(7)	0.5524(9)	0.83(9)
O (11)	0.2263(4)	0.5308(6)	0.8839(8)	1.01(8)
O (12)	0.2214(4)	0.5219(6)	0.3202(8)	0.77(8)
O (13)	0.2253(4)	0.9161(7)	0.3639(8)	1.18(8)

Table 3. *Selected interatomic distances and bond angles*

Si—O distances:

Si(1)—O(7)	1.605 Å	Si(2)—O(8)	1.596 Å
—O(9)	1.614	—O(10)	1.601
—O(11)	1.588	—O(12)	1.656
—O(13)	1.656	—O(13)	1.678
Mean	1.616	Mean	1.633

O—O distances in Si<sub>2</sub>O<sub>7</sub> group:

O(7)—O(9)	2.76 Å	O(8)—O(10)	2.78 Å
O(7)—O(11)	2.72	O(8)—O(12)	2.73
O(7)—O(13)	2.55	O(8)—O(13)	2.52
O(9)—O(11)*	2.59	O(10)—O(12)*	2.64
O(9)—O(13)	2.67	O(10)—O(13)	2.69
O(11)—O(13)	2.48	O(12)—O(13)	2.56

\* Shared edges.

Table 3. (Continued)

C—O distances:			
C(1)—O(1)	1.29 Å	C(2)—O(2)	1.27 Å
—O(3)	1.30	—O(4)	1.29
—O(5)	1.30	—O(6)	1.29
Mean	1.30	Mean	1.28
O—O distances in CO <sub>3</sub> groups:			
O(1)—O(3)*	2.23 Å	O(2)—O(4)*	2.23 Å
O(1)—O(5)	2.27	O(2)—O(6)	2.21
O(3)—O(5)	2.25	O(4)—O(6)	2.23
O—Si—O angles:			
O(7)—Si(1)—O(9)	118.1°	O(8)—Si(2)—O(10)	120.8°
—O(11)	116.8	—O(12)	114.2
—O(13)	102.9	—O(13)	100.6
O(9)—Si(1)—O(11)	108.0	O(10)—Si(2)—O(12)	108.3
—O(13)	109.5	—O(13)	110.2
O(11)—Si(1)—O(13)	99.7	O(12)—Si(2)—O(13)	100.3
Ca—O distances:			
Ca(1)—O(1)	2.367 Å	Ca(2)—O(1)	2.470 Å
—O(2)	2.381	—O(2)	2.436
—O(9)	2.457	—O(4)	2.499
—O(9')	2.387	—O(7)	2.335
—O(10)	2.383	—O(8)	2.322
—O(10')	2.450	—O(9)	2.673
		—O(11)	2.352
Ca(3)—O(2)	2.399 Å	Ca(4)—O(4)	2.435 Å
—O(1)	2.446	—O(5)	2.313
—O(3)	2.440	—O(6)	2.468
—O(8)	2.616	—O(7)	2.403
—O(7)	2.463	—O(11)	2.287
—O(10)	2.676	—O(12)	2.322
—O(12)	2.368		
Ca(5)—O(3)	2.299 Å		
—O(6)	2.369		
—O(5)	2.354		
—O(8)	2.344		
—O(12)	2.557		
—O(11)	2.527		

\* Shared edges.

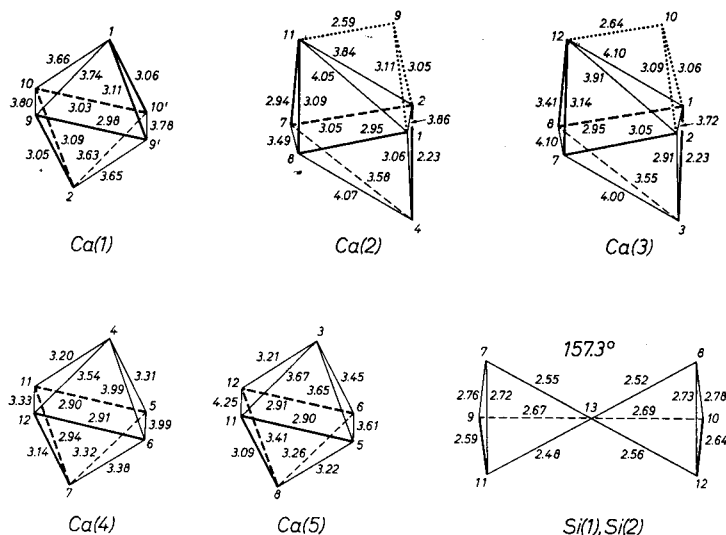


Fig. 1. Schematic diagrams showing the dimensions of the coordination polyhedra in tilleyite. Shared edges are shown by heavy lines. For Ca(2) and Ca(3) the triangular pyramids shown by dotted lines show the change caused by including the seventh-longest Ca—O distance

six more cycles of refinement gave the following agreement factors:  $R = 0.11$  and  $wR = 0.06$  for all reflections.

The observed and calculated structure amplitudes are given in Table 1. Data omitted from the least-squares refinement are marked by an asterisk. Table 2 gives the atomic positional and thermal vibrational parameters, while Table 3 and Fig. 1 give the principal interatomic distances. The standard errors are about  $0.007 \text{ \AA}$  for Si—O and Ca—O distances and about  $0.01 \text{ \AA}$  for C—O and O—O distances.

### Discussion

Figure 2 shows the  $c$ -axis projection of tilleyite in which the  $\text{Si}_2\text{O}_7$  groups are seen end-on as triangles, and each pair of  $\text{CO}_3$  groups superimposes as a single triangle. Each  $\text{CaO}_4$  column of octahedra superimposes in projection to yield the appearance of a single octahedron viewed down a diad axis. The corrugated walls of shared  $\text{Si}_2\text{O}_7$  and  $\text{CaO}_4$  groups lie parallel to  $\{100\}$ . Each wall consists of  $\text{CaO}_4$  columns sharing edges with adjacent pairs of columns and sharing corners with  $\text{Si}_2\text{O}_7$  groups. The corrugated walls are cross-linked by  $\text{CO}_3$  groups sharing corners and edges with the  $\text{CaO}_4$  columns and

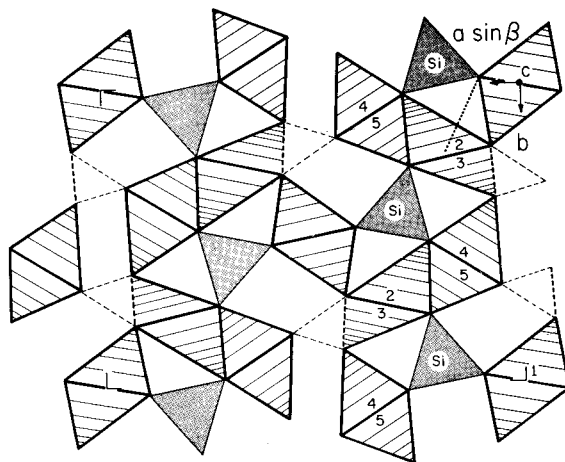


Fig. 2. Idealized projection of the tilleyite structure viewed down the  $c$  axis. The  $\text{Si}_2\text{O}_7$  groups are represented end-on by the stippled triangles. The  $\text{CO}_3$  groups are shown by the broken-line triangles. The  $\text{CaO}_6$  octahedra are viewed down a diad axis; the octahedra for the  $\text{Ca}(2)$  and  $\text{Ca}(3)$  atoms were obtained by omitting the seventh-longest distance shown by the dotted lines (see text). One of the corrugated sheets identified by BELOV consists of the  $\text{Si}_2\text{O}_7$  and  $\text{CaO}_6$  octahedra marked by Si, 2, 3, 4 and 5

by a further type of  $\text{CaO}_4$  column sharing corners with the other structural units.

This description of the structure is idealized since it implicitly ignores the actual geometry. To a first approximation, all atoms in tilleyite except O(13) occur in pairs displaced by about  $c/2$  (see Fig. 8 of SMITH, 1953). The exception, O(13), is the bridging oxygen of the  $\text{Si}_2\text{O}_7$  group, and has no equivalent: in addition, the pairs of Si atoms are only 3.2 Å apart compared to  $c/2 = 3.8$  Å. All of the  $\text{CaO}_6$  octahedra occur in pairs sharing edges to produce columns of  $\text{CaO}_4$  composition lying parallel to  $c$  with a pseudo repeat of  $c/2$ . In addition to the pseudo-halving along  $c$ , there is a pseudo-orthorhombic geometry (but not a pseudo-orthorhombic *symmetry*) as shown by Fig. 10 of SMITH (1953).

There is a further idealization. The coordination polyhedra of the  $\text{Ca}(2)$  and  $\text{Ca}(3)$  atoms are shown as distorted octahedra. Actually each of these Ca atoms has seven oxygen neighbors at 2.3–2.7 Å (Table 2). Although the six atoms ascribed to each octahedron are closer than the rejected ones, all seven are sufficiently close that they must be considered as first neighbors for bonding purposes.

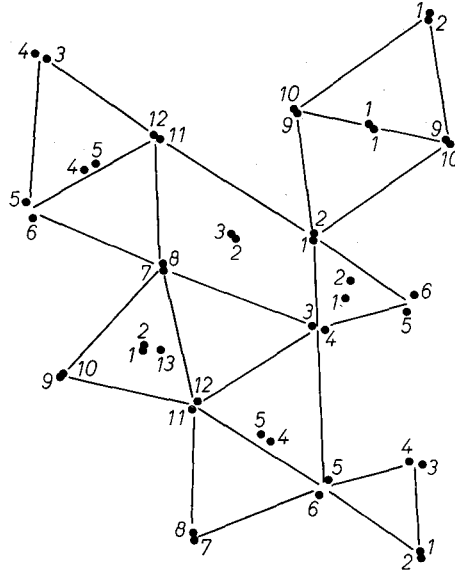


Fig. 3. Comparison of the positions of corresponding atoms as seen in the *c*-axis projection. This diagram corresponds to the upper-right part of Fig. 1. Outlines of mean projections of the polyhedra are shown. The dots show the projections of individual atoms. Note that O(13) does not have a corresponding atom

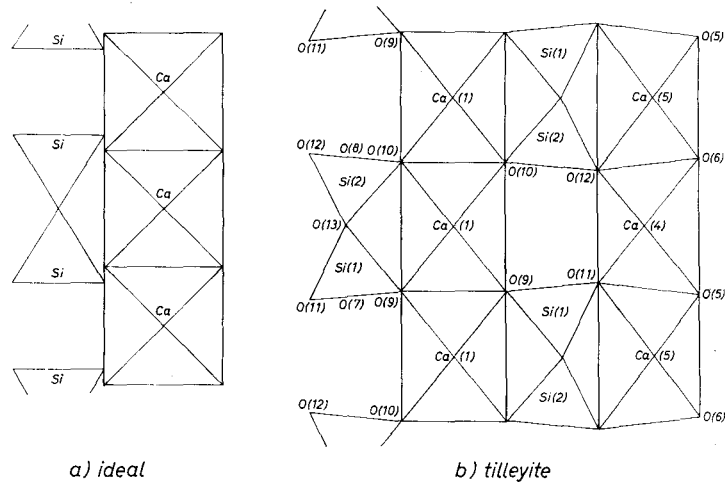


Fig. 4. Comparison of regular  $\text{Si}_2\text{O}_7$  and  $\text{CaO}_6$  groups ( $\text{Si}-\text{O} = 1.62$  and  $\text{Ca}-\text{O} = 2.40 \text{ \AA}$ ) with those found in tilleyite. See text for explanation

The detailed distortions of the structure are very difficult to depict. Figure 3 shows the relative projections of atoms with respect to the idealized drawing of Fig. 2. Figure 1 shows schematically the distortions of the polyhedra in tilleyite. Figure 4 is a simplified diagram demonstrating schematically some of the major distortions in tilleyite.

There are two simple explanations of the distortions: (a) the misfit between the idealized shapes of the  $\text{Si}_2\text{O}_7$  group and the  $\text{CaO}_4$  columns of octahedra, and (b) the shortening of edges shared between polyhedra as expected from electrostatic forces between charged ions. In Fig. 4a the length of an idealized  $\text{Si}_2\text{O}_7$  group (4.3 Å) is considerably greater than the repeat distance (3.4 Å) of undistorted calcium octahedra. The misfit is accommodated in two ways. First of all, sharing of edges between the  $\text{CaO}_6$  groups to form  $\text{CaO}_4$  columns results in a reduction from 3.4–2.9 Å with a concomitant expansion from 3.4–3.8 Å in the perpendicular direction. Secondly, there is a flexing of the  $\text{Si}_2\text{O}_7$  group coupled with distortion of the adjacent  $\text{CaO}_6$  polyhedra. The nature of these distortions is very complex (Figs. 3 and 4b). The Ca(1) polyhedron is relatively restricted since there are centers of symmetry at the center of each edge shared with an adjacent Ca(1) polyhedron down the column. The Ca(4) and Ca(5) polyhedra are suspended between two  $\text{Si}_2\text{O}_7$  groups and four  $\text{CO}_3$  groups, while the Ca(2) and Ca(3) polyhedra are in a very awkward environment which results in 7-fold coordination. As is discussed later, the bridging Si—O—Si angle of an  $\text{Si}_2\text{O}_7$  group is quite variable in crystal structures suggesting that the amount of flexing makes only a small difference to the stability of a crystal structure. The net result of all the factors is that the  $\text{Si}_2\text{O}_7$  groups flex to yield an Si—O—Si angle of  $158^\circ$ . The Ca(1) polyhedra undergo only a little distortion additional to that caused by sharing of edges with other polyhedra. The flexing of the  $\text{Si}_2\text{O}_7$  group causes a severe distortion between the left and right sides of the Ca(4) and Ca(5) polyhedra shown in Fig. 4b. The Ca(2) and Ca(3) polyhedra also undergo complex distortion not shown on Fig. 4b.

The flexing of the  $\text{Si}_2\text{O}_7$  group causes subtle effects on all other structural units, especially the  $\text{CO}_3$  groups, causing them to lose the  $c/2$  relation which would otherwise be possible.

From Fig. 1, it may be seen that the distortions of the  $\text{CaO}_6$  polyhedra correlate strongly with sharing or non-sharing of edges. The Ca(1) polyhedron shares edges only with other Ca polyhedra:

here the effect is very clear since the shared edges of 2.98, 3.03, 3.05, 3.06, 3.09 and 3.11 Å are quite distinct from the unshared edges of 3.65, 3.63, 3.66, 3.74, 3.74, 3.78 and 3.80 Å. For Ca(4) and Ca(5), the effect is less clear since the shared edges range from 2.90–3.41 Å while the unshared edges range from 3.2–4.25 Å. For Ca(2) and Ca(3), the situation is very complex since each polyhedron has one very short edge ( $\sim 2.25$  Å) shared with a CO<sub>3</sub> group, plus the distortion caused by the seventh-near oxygen atom. Packing problems are particularly severe for these two polyhedra but again almost all the shared edges are shorter than the unshared edges.

The two CO<sub>3</sub> groups in tilleyite are equilateral triangles within experimental error. The mean C–O distance of 1.29 Å indicates, as expected, a multiple-bond character for the C–O bond. The oxygen atoms of the carbonate and the pyrosilicate groups form the corners of the Ca polyhedra. This suggests that the C–O and Si–O  $\sigma$ -bonds utilize some  $sp^n$  ( $n \leq 3$ ) hybrid orbitals of the oxygen atoms. Such hybridizations would increase the partial covalent character in some of the Ca–O bonds. Thus some short Ca–O distances (less than the sum of ionic radii, 2.39 Å) could be explained by partial homopolar bonding.

The Si–O distances in the pyrosilicate group are consistent with the  $\pi$ -bonding model proposed by CRUICKSHANK (1961). The Si–O bridge bonds are longer (1.67) than the terminal Si–O distances (1.61). The inner O–O distances (mean 2.58) are shorter than the outer distances (2.71). The O–O distances of the Si<sub>2</sub>O<sub>7</sub> group in four other structures are shown in Fig. 5. The inner distances of the group tend to be shorter than the outer distances. This is well defined in thortveitite (2.60 vs. 2.70) and kornerupine (2.60 vs. 2.69) but is less noticeable for zoisite (2.62 vs. 2.67) and clinozoisite (2.61 vs. 2.67). A possible explanation (SMITH, 1953) is that the distortion is caused by the mean Coulombic forces between ions composing the Si<sub>2</sub>O<sub>7</sub> group: thus the cations tend to pull inwards the outer oxygen atoms, each of which is forced to move apart from the other two members of each outer triangular group in order to maintain a near-constancy of Si–O distances. In addition there are forces from outside the Si<sub>2</sub>O<sub>7</sub> group, for example those involving edge sharing. In CRUICKSHANK's  $\pi$ -bonding model the short inner O–O distances arise from lesser electrostatic repulsions between the bridging and the non-bridging oxygen atoms as against the stronger repulsions between the non-bridging oxygen atoms (MCDONALD and CRUICKSHANK, 1967).

Table 4. Selected dimensions of the Si<sub>2</sub>O<sub>7</sub> group in some structures

Structure	Mean interatomic distance		$\Delta d$ (bridge – peripheral bond length)	Si–O–Si bridging angle	Reference
	Si–O (bridge)	Si–O (peripheral)			
I. Thortveitite	1.6045(5) Å	1.628(1) Å	– 0.023(1) Å	180.0(0)°	PREWITT (personal communication)
II. Ba <sub>3</sub> Si <sub>4</sub> Nb <sub>6</sub> O <sub>26</sub>	1.599(6)	1.629(7)	– 0.030(9)	180°	SHANNON and KATZ (1970)
III. Zoisite	1.633(10)	1.620(6)	+ 0.013(10)	172.6(8)	DOLLASE (1968)
IV. Clinozoisite	1.628(4)	1.617(4)	+ 0.011(5)	164.3(5)	DOLLASE (1968)
V. Tilleyite	1.667(4)	1.610(4)	+ 0.057(6)	157.3(4)	this work
VI. Kornerupine	1.65(1)	1.61(1)	+ 0.04(1)	146.2(5)	MOORE and BENNETT (1968)
VII. Hardystonite	1.649(3)	1.607(3)	+ 0.042(4)	138.5(3)	LOUISNATHAN (1969)

Standard errors given in brackets to same decimal level.



There has been considerable speculation on the size of the Si—O—Si angle. The observed variation is from  $180^\circ$  to about  $135^\circ$ . LIEBAU (1961) suggested that the Si—O—Si angle must be less than  $180^\circ$  in conformity with an expected partial covalent character of bonding in silicates. In CRUICKSHANK'S  $\pi$ -bonding model an angle near  $180^\circ$

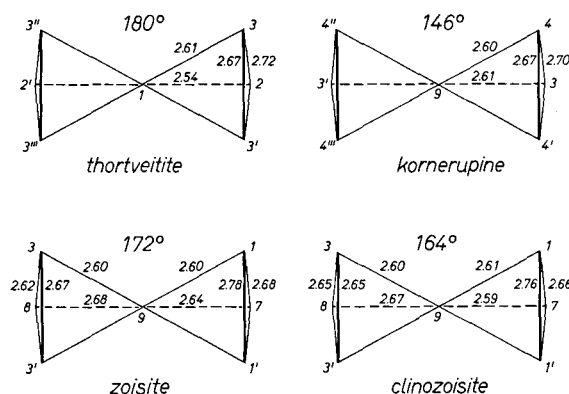


Fig. 5. Schematic diagrams showing the dimensions of the coordination polyhedra in four silicates. The Si—O—Si bridge angle is also shown

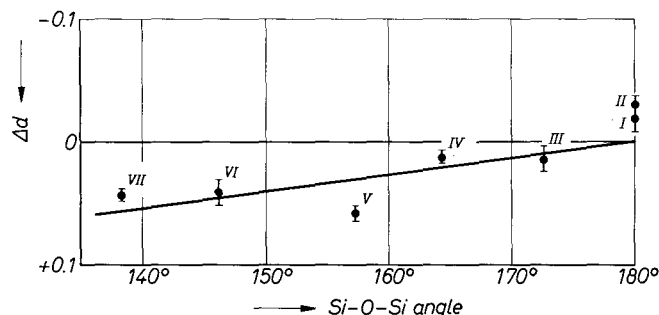


Fig. 6. Correlation between the Si—O—Si bridge angle and the difference ( $\Delta d$ ) in the bridge and peripheral bond lengths. Errors in  $\Delta d$  ( $\sqrt{\sigma_{br}^2 + \sigma_{per}^2}$ ) are also shown in the diagram. Numerals on the plot refer to those in Table 4

would enable the bridging oxygen to participate in both  $\pi$  systems, and the Si—O bridge bond would tend to become shorter than the terminal bonds. LAZAREV'S (1964) investigation supported this hypothesis, and he suggested that for large Si—O—Si angles the repulsion between the two silicon atoms is minimized because of increased

electron density in the  $\pi$  bond. In Table 4 and Fig. 5 are given the dimensions of seven out of many structures that contain the pyrosilicate group. The variation of the Si—O—Si angle with the difference in the lengths of the bridge bond and mean peripheral bond is shown in Fig. 6. The decrease in the difference as the Si—O—Si angle increases is consistent with the  $\pi$ -bonding model, but the correlation factor is obviously low. BROWN and GIBBS (1970) reported a similar correlation in their analysis of several silicate structures. In tilleyite the observed difference of 0.057(6) Å for an angle of 157° is somewhat large.

A straightforward explanation for the size of the Si—O—Si angle can be given in terms of packing relationships between the Si<sub>2</sub>O<sub>7</sub> group and the neighboring polyhedra. For example, the angle of 157° in tilleyite can be justified plausibly by the geometrical requirements for linkage to the columns of Ca octahedra, while the higher angle in zoisite appears to result from the spatial requirements resulting from the suspension of the Si<sub>2</sub>O<sub>7</sub> group between the columns of AlO<sub>6</sub> octahedra.

Nevertheless it would be surely wrong to believe that the flexing of bridging angle has no effect on the contribution of the Si<sub>2</sub>O<sub>7</sub> group to the internal energy.

We have shown that the principal distortions in the calcium-oxygen octahedra and the silicon-oxygen tetrahedra are mostly explainable in terms of PAULING'S (1960) arguments regarding chemical bonding in complex ionic structures. Within the Si<sub>2</sub>O<sub>7</sub> group the variation of individual bond lengths can be satisfactorily accounted for in terms of CRUICKSHANK'S  $\pi$ -bonding theory, but valence-balancing (ZACHARIASEN, 1963*b*) could also provide an interpretation. As has been recognized by PANT and CRUICKSHANK (1968) the two theories are not exclusive. However it must be emphasized that neither the  $\pi$ -bonding theory nor the method of valence balancing examines anything more than the first-nearest neighbors in a structure for describing the chemical bond. Such an approach is certainly far from complete in a complex structure like tilleyite.

#### Acknowledgements

We thank the Petroleum Research Fund administered by the American Chemical Society for a grant-in-aid, and the National Science Foundation for grant G-1658. Professors P. B. MOORE and E. FLEISCHER kindly assisted with the PAILRED diffractometer. Professor G. V. GIBBS made helpful suggestions on the manuscript.

## References

- N. V. BELOV (1963), *Crystal chemistry of large-cation silicates*. [Transl. from Russian.] Consultants Bureau, New York.
- G. E. BROWN and G. V. GIBBS (1970), Stereochemistry and Al/Si ordering in the tetrahedral positions of silicates. *Amer. Mineral.* **55**, 1587–1607.
- D. T. CROMER (1965), Anomalous dispersion corrections computed from self-consistent field relativistic Dirac-Slater wave functions. *Acta Crystallogr.* **18**, 17–23.
- D. W. J. CRUICKSHANK (1961), The role of 3*d*-orbitals in  $\pi$ -bonds between (a) silicon, phosphorus, sulphur, or chlorine and (b) oxygen or nitrogen. *J. Chem. Soc.* **1961**, 5486–5504.
- W. A. DOLLASE (1968), Refinement and comparison of the structures of zoisite and clinozoisite. *Amer. Mineral.* **53**, 1882–1898.
- A. N. LAZAREV (1964), Polymorphism of molecules and complex ions in oxygen compounds. Report 1. Nature of the Si–O–Si bonds and values of valence angles of oxygen. *Bull. Acad. Sci. USSR, Division Chem. Sci.* **1**, 218–223.
- F. LIEBAU (1961), Untersuchungen über die Größe des Si–O–Si-Valenzwinkels. *Acta Crystallogr.* **14**, 1103–1109.
- S. J. LOUISNATHAN (1969), Ph. D. dissertation, University of Chicago, Chicago, Illinois.
- W. S. McDONALD and D. W. J. CRUICKSHANK (1967), A reinvestigation of the structure of sodium metasilicate, Na<sub>2</sub>SiO<sub>3</sub>. *Acta Crystallogr.* **22**, 37–43.
- P. B. MOORE and J. M. BENNETT (1968), Kornerupine: its crystal structure. *Science* **159**, 524–526.
- A. K. PANT and D. W. J. CRUICKSHANK (1968), The crystal structure of  $\alpha$ -Na<sub>2</sub>Si<sub>2</sub>O<sub>5</sub>. *Acta Crystallogr.* **B24**, 13–19.
- L. PAULING (1960), *The nature of the chemical bond*. Cornell Univ. Press.
- J. SHANNON and L. KATZ (1970), The structure of barium silicon niobium oxide, Ba<sub>3</sub>Si<sub>4</sub>Nb<sub>6</sub>O<sub>26</sub>: A compound with linear silicon-oxygen-silicon groups. *Acta Crystallogr.* **B26**, 105–109.
- J. V. SMITH (1951), Ph. D. thesis, University of Cambridge.
- (1953), The crystal structure of tilleyite. *Acta Crystallogr.* **6**, 9–18.
- W. H. ZACHARIASEN (1963*a*), The secondary extinction correction. *Acta Crystallogr.* **16**, 1139–1144.
- (1963*b*), The crystal structure of monoclinic metaboric acid. *Acta Crystallogr.* **16**, 385–389.